Cell Reports
Article

The BCL6 RD2 Domain Governs Commitment of Activated B Cells to Form Germinal Centers

Chuanxin Huang,[1] David G. Gonzalez,[2] Christine M. Cote,[2] Yanwen Jiang,[1] Katerina Hatzi,[1] Matt Teater,[1] Kezhi Dai,[3] Timothy Hla,[3] Ann M. Haberman,[2,*] and Ari Melnick[1,*]
[1]Division of Hematology and Oncology, Department of Medicine, Weill Cornell Medical College, New York, NY 10065, USA
[2]Department of Laboratory Medicine and Immunobiology, Yale University, New Haven, CT 06520, USA
[3]Department of Pathology and Laboratory Medicine, Weill Cornell Medical College, New York, NY 10065, USA
*Correspondence: ann.haberman@yale.edu (A.M.H.), amm2014@med.cornell.edu (A.M.)
http://dx.doi.org/10.1016/j.celrep.2014.07.059

SUMMARY

To understand how the Bcl6 transcriptional repressor functions in the immune system, we disrupted its RD2 repression domain in mice. *Bcl6*RD2^{MUT} mice exhibit a complete loss of germinal center (GC) formation but retain normal extrafollicular responses. *Bcl6*RD2^{MUT} antigen-engaged B cells migrate to the interfollicular zone and interact with cognate T helper cells. However, these cells fail to complete early GC-commitment differentiation and coalesce as nascent GC aggregates. Bcl6 directly binds and represses trafficking receptors S1pr1 and Gpr183 by recruiting Hdac2 through the RD2 domain. Deregulation of these genes impairs B cell migration and may contribute to GC failure in *Bcl6*RD2^{MUT} mice. The development of functional GC-T$_{FH}$ cells was partially impaired in *Bcl6*RD2^{MUT} mice. In contrast to *Bcl6*$^{-/-}$ mice, *Bcl6*RD2^{MUT} animals experience no inflammatory disease or macrophage deregulation. These results reveal an essential role for RD2 repression in early GC commitment and striking biochemical specificity in Bcl6 control of humoral and innate immune-cell phenotypes.

INTRODUCTION

In response to T cell-dependent (TD) antigen stimulation, antigen-specific B cells migrate to the periphery of B cell follicles and interfollicular zones of secondary lymphoid organs, where they interact with cognate T helper cells within 1–3 days (Kerfoot et al., 2011; Okada et al., 2005; Qi et al., 2008). After then, B cells can follow one of three alternative fates by differentiating into extrafollicular plasma cells, follicular germinal center (GC) B cells, or recirculating early memory B cells (McHeyzer-Williams et al., 2012). GC B cells undergo massive clonal expansion, somatic hypermutation, and class switch recombination, after which selected clones undergo differentiation into memory B cells and long-lived plasma cells (Allen et al., 2007; Victora and Nussenzweig, 2012). T follicular helper (T$_{FH}$) cells express the chemokine receptor CXCR5 and costimulatory molecule PD-1 at high levels and specialize in providing help to B cells during the humoral immune response (Crotty, 2011). Antigen-presenting dendritic cells mediate the initiation of T$_{FH}$ cell differentiation at early time points after immunization (Choi et al., 2011; Goenka et al., 2011). Interactions with cognate B cells, especially GC B cells within GCs, are critical for further polarization, maintenance, and function of T$_{FH}$ cells at later stages of the immune response (Choi et al., 2011; Kerfoot et al., 2011; Kitano et al., 2011). Thus, the reciprocal development of GC B cells and T$_{FH}$ cells is crucial for establishment of the GC reaction, including the formation of high-affinity antibody and the generation of long-lived plasma cells.

The Bcl6 transcriptional repressor is a master regulator of the GC reaction required for development of both GC B cells and T$_{FH}$ cells, respectively (Dent et al., 1997; Fukuda et al., 1997; Johnston et al., 2009; Nurieva et al., 2009; Ye et al., 1997; Yu et al., 2009). In addition, Bcl6 plays a key role in suppressing inflammatory cytokine expression in macrophages (Toney et al., 2000). *Bcl6*-deficient (*Bcl6*$^{-/-}$) mice in addition to failing to form GCs are sickly and die within weeks from a lethal inflammatory syndrome primarily driven by macrophages with secondary contributions from Th2 and Th17 cells (Mondal et al., 2010; Toney et al., 2000). However, from a mechanistic standpoint the function of *Bcl6* is poorly understood outside of the context of already established GC B cells. Bcl6 enables proliferation and tolerance of DNA damage by silencing DNA damage sensing and cell cycle checkpoint genes, and it also delays plasma cell differentiation by repression of critical GC exit and plasma cell differentiation genes (Bunting and Melnick, 2013; Klein and Dalla-Favera, 2008). However, *Bcl6*$^{-/-}$ mice display a complete loss of GC formation with no evidence of the capacity to establish nascent GC clusters (Dent et al., 1997; Fukuda et al., 1997; Ye et al., 1997), suggesting that Bcl6 might have biological functions prior to GC formation. Indeed, Bcl6 protein is upregulated in early GC-committed B cells (i.e., "pre-GC B cells") outside GCs 3–5 days after immunization (Kerfoot et al., 2011; Kitano et al., 2011) and plays an essential role in maintaining interactions with T$_{FH}$ cell as well as subsequent migration and clustering into GC structures, at least in part through repressing the expression of *Gpr183*, encoding the G protein-coupled receptor Ebi2 (Kitano et al., 2011; Shaffer et al., 2000).

Bcl6 functions as a transcription repressor via its N-terminal BTB domain and middle "second repression," or "RD2" domain (Chang et al., 1996; Seyfert et al., 1996). A loss of function of the BCL6 BTB domain markedly impairs survival and proliferation of mature GC B cells in a B cell intrinsic manner, with no effects on T cells or macrophages (Huang et al., 2013). Notably, unlike *Bcl6*$^{-/-}$ B cells, BTB-deficient B cells still form GCs although their numbers and sizes are markedly reduced. This discrepancy illustrates our incomplete understanding of the molecular underpinnings of Bcl6-mediated GC B cell development and suggests that other functions of Bcl6 are dominantly involved in modulating early pre-GC B cell fate.

In this study we generated mice in which the native *Bcl6* locus was engineered to produce a form of Bcl6 containing a mutant RD2 domain that disrupts its repressor function. We found that RD2 domain is essential for pre-GC B cell differentiation and clustering into nascent GC within follicles, in part through repressing key trafficking receptors S1pr1 and Gpr183 by recruiting Hdac2. Thus, these findings implicate the Bcl6 RD2 domain as defining the fate of activated B cells toward the GC phenotype, which is mechanistically distinct from its role in enabling proliferation and survival upon induction of the proliferative burst within GCs. The activities of Bcl6 can thus be parsed out into unique biochemical elements, each contributing different actions to the functionality of immune system.

RESULTS

Generation and Characterization of Bcl6 RD2 Mutant Knockin Mice

To more precisely localize the repressor function of the Bcl6 RD2 domain, we first mapped the minimal region sufficient for its transcription repression activity. The full-length RD2, which spans the region from the BTB domain to the zinc finger domain (amino acids 129 to 519), mediated strong transcriptional repression similar to the Bcl6 BTB domain (Figures S1A and S1B). Progressive truncation yielded a 45-amino acid region (amino acids 350 to 395) as the minimal domain containing a similar repressive effect as full-length RD2 (Figure S1B). This 45 amino acid domain encompassed a known, functionally important KKYK motif (amino acids 387 to 390). The introduction of K387Q, K388Q, and K390Q substitutions (lysine at 387, 388, and 390 to glutamine), mimics of acetylation of the KKYK, completely abrogated transcriptional repression mediated by either the 45-amino acid region or the full-length RD2 domain (Figure S1B).

It was reported that the Bcl6 middle region containing the RD2 domain binds to histone deacetylase 2 (HDAC2), MTA3-NuRD complex, and CtBP (Bereshchenko et al., 2002; Fujita et al., 2004; Mendez et al., 2008). We found that wild-type minimal 45-animo acid RD2 domain, but not its QQYQ mutant form, interacts with HDAC2 as well as NuRD subunits Mi-2 and MTA3, but not CtBP, in coimmunoprecipitation assays (Figure S1C). Reporter assays showed that both HDAC2 and MTA3 contribute to the repressor function of the minimal RD2 domain (Figure S1D). Collectively, these results show that a 45-amino acid domain mediates the autonomous repressor function of the Bcl6 RD2 domain and its activity can be disrupted through mutations of key lysine residues.

We next utilized a homologous recombination strategy to introduce K387Q, K388Q, and K390Q point mutations into the native *Bcl6* locus in mice (Figures S1E and S1F). This enabled us to generate a Bcl6 RD2 mutant knockin mouse strain (called "*Bcl6*RD2^{MUT}" henceforth; Figure S1G). In contrast to *Bcl6*$^{-/-}$ mice, *Bcl6*RD2^{MUT} mice were born at the expected Mendelian ratios and were grossly normal in growth and survival. Expression of the mutant Bcl6 gene product was confirmed by immunoblotting and sequencing (Figures S1H and S1I). Quantitative chromatin immunoprecipitation (QChIP) assays demonstrated that endogenous *Bcl6*RD2^{MUT} protein binds to target genes in primary murine macrophages to a similar extent as WT Bcl6 protein and retains the ability to recruit SMRT corepressors through the BTB domain (Figure S1J).

*Bcl6*RD2^{MUT} Mice Display a Normal Extrafollicular Response but a Complete Abrogation of the GC Reaction

Bcl6$^{-/-}$ mice display a reduction of immature B cells in bone marrow and mature B cells in spleen (Duy et al., 2010). However, *Bcl6*RD2^{MUT} display normal B cell development prior to the GC stage (Figures S1K and S1L) and form normal splenic primary lymphoid follicles (Figure S1M). Next, we studied the role of the Bcl6 RD2 domain in the TD antigen immune response. TD antigen stimulation first induces an extrafollicular response to give rise to an early wave of low-affinity antibodies. We immunized a cohort of age-matched WT and *Bcl6*RD2^{MUT} mice with sheep red blood cells (SRBCs), a T cell-dependent antigen. *Bcl6*RD2^{MUT} and WT mice produced a similar amount of splenic NP-specific plasmablast or plasma cells (NP^{+}CD138^{+}B220$^{lo\text{-}neg}$) and splenic IgM and IgG NP-specific antibody secreting cells at day 7 after immunization with 4-hydroxy-3-nitrophenylacetyl conjugated to chicken gamma globulin (NP-CGG), a well-defined TD antigen (Figures S2A and S2B).

At later time points, TD antigen immunization induces the GC (follicular) response to produce high-affinity antibodies. Remarkably, *Bcl6*RD2^{MUT} exhibited a complete absence of any GCs in B cell follicles of spleens at day 5,10, and 14 after SRBC immunization, revealed by immunochemistry (Figure 1A), similar to *Bcl6*$^{-/-}$ mice. A complete loss of GCs was also observed in Peyer's patches (Figure 1A). Accordingly, flow cytometry analysis showed that CD38$^{lo\text{-}neg}$Fas^{+} GC B cells were virtually undetectable in immunized *Bcl6*RD2^{MUT} mice at day 10 after SRBC immunization (<0.1%; Figure 1B), identical to *Bcl6*$^{-/-}$ mice. Both CXCR5^{hi}PD1^{hi} GC-T_{FH} and CXCR5^{int}PD1^{int}T_{FH} were profoundly reduced in immunized *Bcl6*RD2^{MUT} mice (0.7% ± 0.2% and 2.7% ± 0.4%, respectively; $p < 0.01$ versus WT; Figure 1C). As expected, GC-T_{FH} and T_{FH} cells were virtually absent in immunized *Bcl6*$^{-/-}$ mice (<0.1 and <1.0, respectively; Figure 1C). Similar defects were detected in *Bcl6*RD2^{MUT} mice challenged with NP-CGG (Figure S2C). *Bcl6*RD2^{MUT} mice displayed progressively lower levels of total NP-specific immunoglobulins after day 7 after NP-CGG immunization, most strikingly at day 32 (Figure S2D). The titers of all high-affinity NP-specific immunoglobulin isotypes, captured by NP4, were significantly lower in *Bcl6*RD2^{MUT} than WT mice at day 32 ($p < 0.01$; Figure S2E). The ratio of titers of high-affinity IgG1 to those of total IgG1, which indicates antibody maturation, was also lower in *Bcl6*RD2^{MUT} than WT mice ($p < 0.01$; Figure S2F). Collectively,

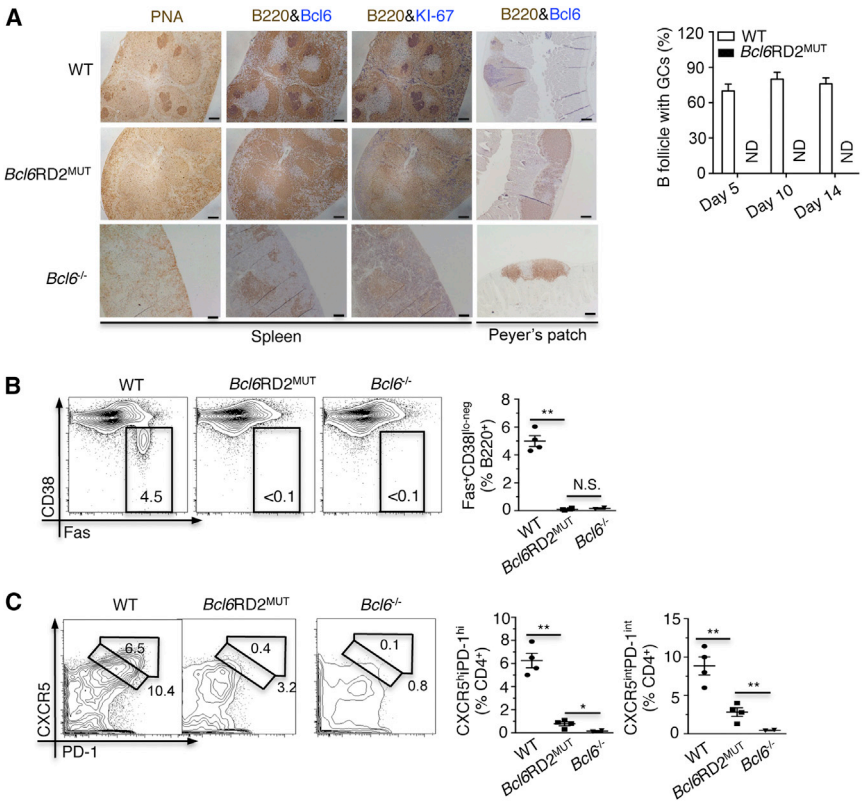

Figure 1. Complete Loss of GCs in *Bcl6*RD2^{MUT} Mice

(A–C) WT and *Bcl6*RD2^{MUT} mice were immunized i.p. with SRBCs.

(A) Representative immunohistochemical staining for PNA, B220, and Bcl6 on paraffin-embedded serial spleen sections and Peyer's patches. Scale bars, 200 μm. ND, not detected; n = 3 each time point per group.

(B and C) Flow cytometry of murine splenic cells 10 days after immunization. The adjacent dot plots indicate the percentage of Fas$^+$ CD38$^{lo\text{-}neg}$ GC B cells among total B cells (B), as well as CXCR5^{h}iPD1^{hi} GC-T$_{FH}$ and CXCR5^{int}PD1^{int} T$_{FH}$ cells among total CD4$^+$ T cells (C). N.S., not significant; *p < 0.05 and **p < 0.01 (two-tailed t test).

these data demonstrate that transcriptional repression through the RD2 domain of Bcl6 is required for the GC response and high-affinity immunoglobulin maturation, but dispensable for the extrafollicular response.

The Bcl6 RD2 Domain Is Essential for GC B, but Not GC-T$_{FH}$, Cell Formation

The requirement of *Bcl6* for GC formation is due to its dual and cell autonomous role in the development of both GC B cells and T$_{FH}$ cells. Moreover, the development of these two cell types is interdependent. Thus, the loss of GC B cells and T$_{FH}$ cells in *Bcl6*RD2^{MUT} mice could be caused by B cell and/or T cell deficiency. To determine the potential contribution of these cell types to the *Bcl6*RD2^{MUT} phenotype, we generated mixed bone marrow chimeras by transferring 50% of congenic CD45.1$^+$ WT bone marrow cells together with 50% of CD45.2$^+$ bone marrow cells from WT, *Bcl6*$^{-/-}$, or *Bcl6*RD2^{MUT} mice into sublethally irradiated Rag1$^{-/-}$ mice, which were then immunized after reconstitution (Figure 2A). As expected, CD45.2$^+$ *Bcl6*$^{-/-}$ donor cell-derived GC B cells, GC-T$_{FH}$ cells, and T$_{FH}$ cells were essentially absent from CD45.1$^+$ WT and CD45.2$^+$*Bcl6*$^{-/-}$ mixed chimeras ($p < 0.01$; Figures 2B and 2C). Analysis of CD45.2$^+$ *Bcl6*RD2^{MUT} chimeras revealed a complete absence of CD45.2$^+$ GC B cells (Figure 2B), but yet still formed a normal number of CD45.2$^+$ T$_{FH}$ cells ($p > 0.05$) and approximately 60% CD45.2$^+$ GC-T$_{FH}$ cells compared with WT donor T cells ($p < 0.05$; Figure 2C), which was similar to a hypomorphic defect observed in *Bcl6*$^{+/-}$ T cells (Yu et al., 2009). Together, these results indicate that RD2-dependent repression is essential for the generation of GC B cells, but were more dispensable for GC-T$_{FH}$ cell differentiation.

RD2-Deficient B Cells Are Unable to Support a Functional GC Reaction

We next examined whether the functional defects in GC formation in *Bcl6*RD2^{MUT} mice were cell intrinsic to GC B cells and/or GC-T$_{FH}$ cells. For this we reconstructed chimeras by transferring μMT bone marrow (80%) along with bone marrow cells (20%) from WT, *Bcl6*RD2^{MUT}, or *Bcl6*$^{-/-}$ mice into sublethally irradiated Rag1$^{-/-}$ recipients (Figure 3A). The μMT bone marrow cells provide a source of normal T cells, but not B cells, thus all B cells in these chimeras originate from tested donor bone marrow. GC B cells were virtually absent in *Bcl6*RD2^{MUT} mixed chimeras 10 days after immunization with SRBCs (Figure 3B). Accordingly, titers of total NP specific antibodies (binding NP26) were reduced by 88% and the titers of high-affinity IgG1 NP-specific antibodies (binding NP4) were reduced by 95% in *Bcl6*RD2^{MUT} versus WT mixed chimeras ($p < 0.05$ versus WT) 21 days after NP-CGG immunization (Figure 3C). Notably, the impairment in GC B cell numbers and titers of high-affinity antibodies were indistinguishable between *Bcl6*RD2^{MUT} and *Bcl6*$^{-/-}$ mixed chimeras (Figure 3C), demonstrating that B cells absolutely require the Bcl6 RD2 domain for GC formation and functionality.

RD2-Deficient T Cells Are Modestly Impaired in Supporting a Functional GC Reaction

The Bcl6 RD2 domain appears to play a relatively limited role in instructing GC-T$_{FH}$ cell differentiation (Figure 2C). To determine whether these cells were functionally impaired in driving humoral immunity, chimeras were generated by transferring a 4:1 mixture of *Tcrb*$^{-/-}$*Tcrd*$^{-/-}$ and WT, *Tcrb*$^{-/-}$*Tcrd*$^{-/-}$ and *Bcl6*RD2^{MUT}, or *Tcrb*$^{-/-}$*Tcrd*$^{-/-}$ and *Bcl6*$^{-/-}$ bone marrow cells into sublethally irradiated Rag1$^{-/-}$ recipients (Figure 3D). In these chimeras the *Tcrb*$^{-/-}$*Tcrd*$^{-/-}$ strain contributes normal B cells, whereas T cells are derived from tested WT,

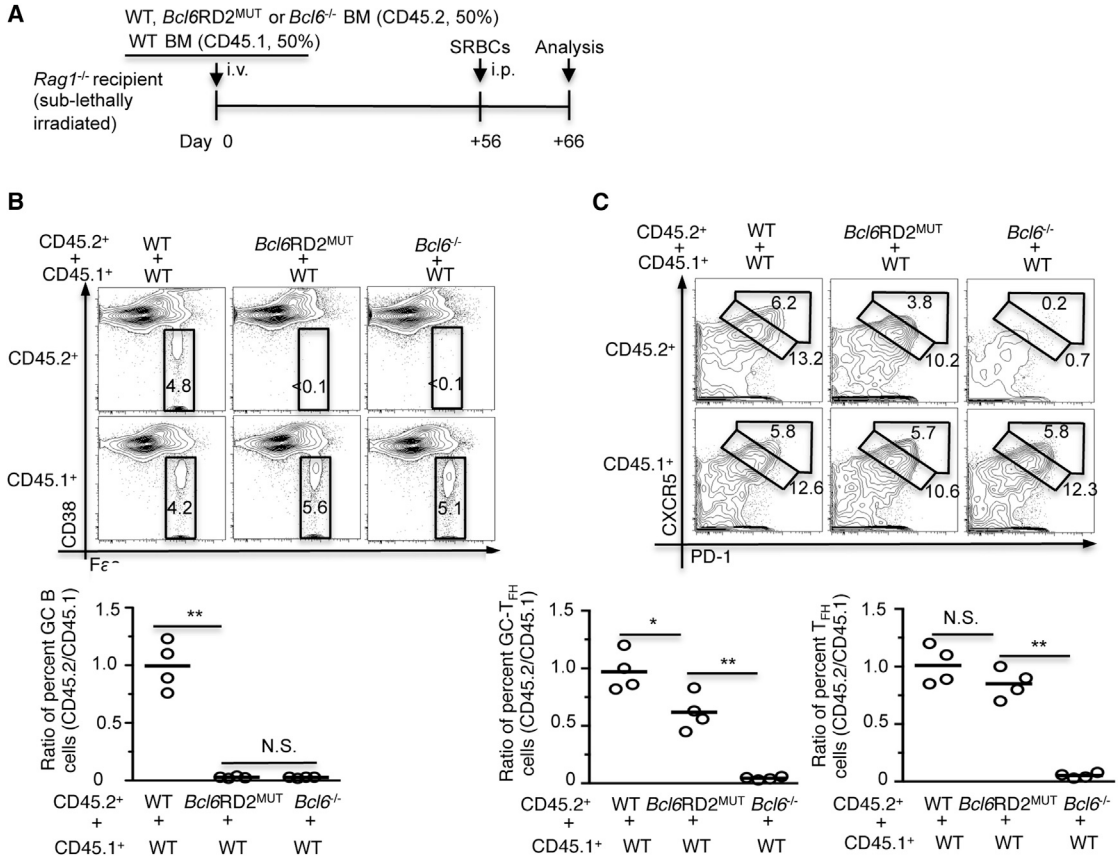

Figure 2. Intrinsic Defects in GC B, but Not T_{FH}, Cells in *Bcl6*RD2^{MUT} Mice

(A) Schematic outline of generation of mixed chimeras and immunization.

(B and C) Flow cytometry and adjacent dot plots showing percent of Fas+ CD38$^{lo\text{-}neg}$ GC B cells among live B220+ cells (B) and percent of CXCR5^{hi}PD^{hi} GC-T_{FH} and CXCR5^{int}PD1^{int} T_{FH} cells among live CD4$^+$ cells from CD45.1 or CD45.2 donors (C). The ratio was calculated by dividing percent GC B cells or T_{FH} cells from CD45.2 donor by that from CD45.1 donor. Each symbol represents an individual mouse, and small horizontal lines indicate means. Data are from three independent experiments with four mice per genotype. N.S., not significant; *p < 0.05 and *p < 0.01 (two-tailed t test).

*Bcl6*RD2^{MUT}, or *Bcl6*$^{-/-}$ marrow cells. Eight weeks after reconstitution, animals were immunized with SRBCs or NP-CGG. The frequency of GC B cells among splenic B cells in *Tcrb*$^{-/-}$*Tcrd*$^{-/-}$ and WT mixed chimeras was 3.1% ± 0.3% 10 days after SRBC immunization, whereas GC B cells were essentially undetectable in *Bcl6*$^{-/-}$ mixed chimeras (<0.1%; Figure 3E). Notably, *Bcl6*RD2^{MUT} mixed chimeras displayed a mild, albeit significant, reduction of GC B cells, with a frequency of 1.8% ± 0.6% ($p < 0.05$ versus WT; Figure 3E). The titers of total NP-specific IgG1 antibodies in NP-CGG immunized *Bcl6*RD2^{MUT} mixed chimeras were indistinguishable to WT (Figure 3F). In contrast, the titers of high-affinity NP-specific IgG1 antibodies in *Bcl6*RD2^{MUT} chimers were significantly reduced compared with WT chimeras ($p < 0.05$; one-tailed t test; Figure 3F). However, antibody titers were still significantly higher in *Bcl6*RD2^{MUT} mixed chimeras as compared with *Bcl6*$^{-/-}$ chimeras ($p < 0.05$; Figure 3F). Taken together, these data indicate that inactivation of the RD2 domain leads to a T_{FH} functional defect, which, although significant, is much less severe than that caused by *Bcl6* knockout.

To gain some insight into the basis of this modest defect, we isolated CD45.2$^+$ Bcl6RD2^{MUT} GC-T_{FH} and CD45.1$^+$ WT counterparts from SRBC-immunized mixed CD45.1$^+$ WT and CD45.2$^+$ WT chimeras (Figure S3A) and examined the expression of several key T_{FH} cell-associated genes including *IL-21* and *Blimp1*. IL-21 is expressed by T_{FH} cells and signals to B cells to regulate GC responses (Linterman et al., 2010; Zotos et al., 2010). *Blimp1* is an important Bcl6 direct target and antagonistic regulator of T_{FH} cell differentiation (Johnston et al., 2009). Notably, Bcl6RD2^{MUT} GC-T_{FH} expressed a lower abundance of *Il-21* and higher levels of *Blimp1* compared with WT counterparts (Figure S3B). The Bcl6 RD2 domain has been reported to repress Blimp1 transcription in B cells (Fujita et al., 2004). We next analyzed whether RD2 deficiency might directly impair Bcl6-dependent repression of Blimp1 transcription in T cells using a luciferase reporter driven by the *Blimp*1β promoter, which contains the consensus Bcl6 binding site (Figure S3C) that is the major binding site for Bcl6 at *Blimp*1 locus (Hatzi et al., 2013). Indeed, we observed that RD2 deficiency significantly impaired Bcl6-mediated repression of the *Blimp*1β promoter in T cells (Figure S3D).

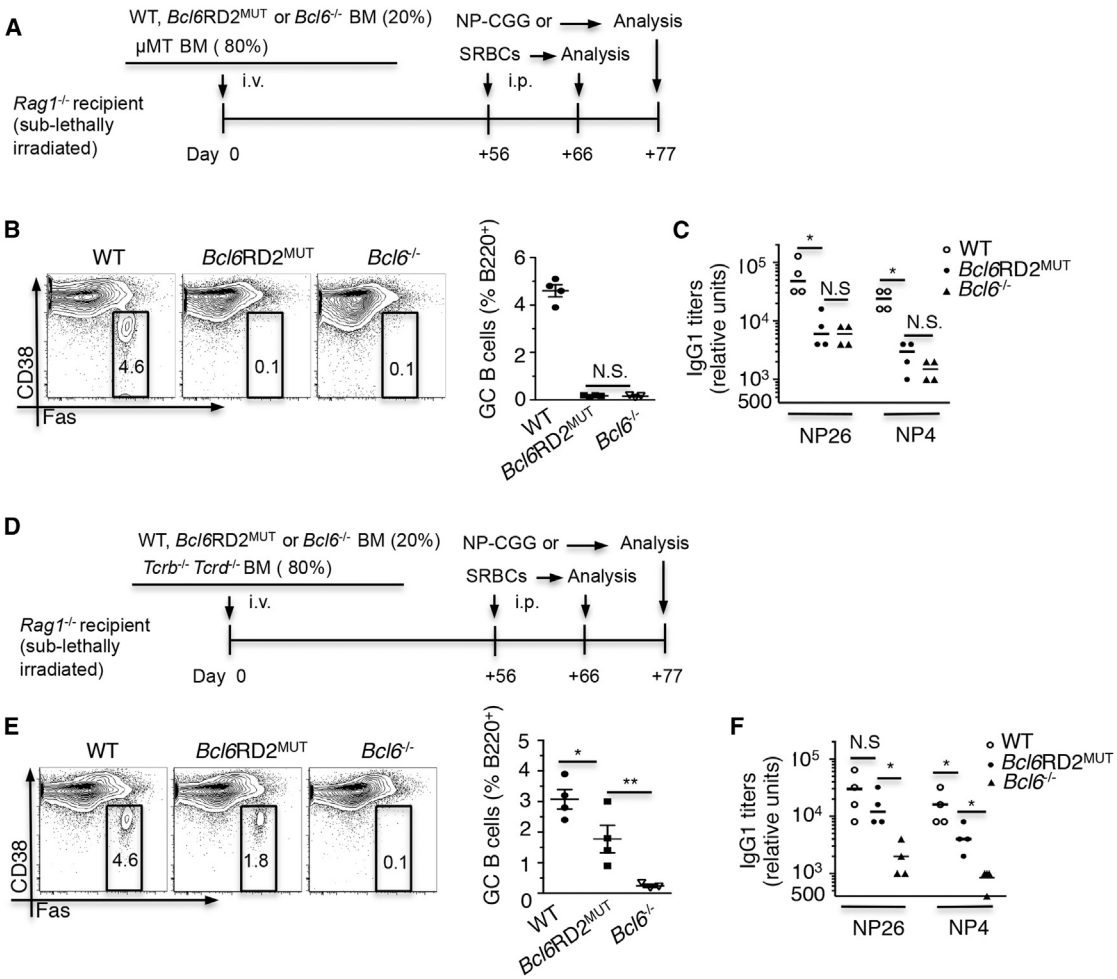

Figure 3. Severely Impaired Function of RD2-Deficient GC B Cells and Modest Defect in T Cells

(A) Schematic outline of generation of μMT chimeras and immunization.

(B) Flow cytometry of FAS+ CD38$^{lo\text{-}neg}$ GC B cells among live splenic B220+ cells from SRBC-immunized μMT chimeras.

(C) ELISA of NP-specific IgG1 in sera from NP26-CGG-immunized μMT chimeras.

(D) Schematic outline of generation of *Tcrb*$^{-/-}$*Tcrd*$^{-/-}$ chimeras and immunization.

(E) Flow cytometry of FAS^{+}CD38$^{lo\text{-}neg}$ GC B cells among live splenic B220^{+} cells from SRBC-immunized *Tcrb*$^{-/-}$*Tcrd*$^{-/-}$ chimeras.

(F) ELISA of NP-specific IgG1 in sera from NP-CGG-immunized *Tcrb*$^{-/-}$*Tcrd*$^{-/-}$ chimeras.

Each symbol represents an individual mouse, and small horizontal lines indicate means (B, C, E, and F). Data are from two independent experiments with four mice per genotype. RU, relative units; N.S., not significant; *p < 0.05 and **p < 0.01 (two-tailed t test).

The Early Phase of the *Bcl6*RD2^{MUT} B Cell Response Appears Normal

The striking and complete defect in GC formation observed in Bcl6RD2^{MUT} mice is similar to Bcl6$^{-/-}$ mice and different than the Bcl6 BTB mutant mouse strain, in which GCs are still observed at late time points (day 10) (Huang et al., 2013), suggesting that the functional defect of *Bcl6*RD2^{MUT} B cells occurs at an early time point of GC development (day 4) before the onset of rapid population expansion of GC B cells (Calado et al., 2012). Indeed, SRBC-immunized BTB mutant mice formed robust early GC clusters in spleen and Peyer's patches at day 4, whereas in *Bcl6*RD2^{MUT} mice the ability to develop early GC clusters was completely abrogated (Figure S4A).

We next examined the early stages of *Bcl6*RD2^{MUT} B cell development in response to TD immunization. To this end, *Bcl6*RD2^{MUT} mice were bred with a GFP-expressing strain and their offspring further crossed to MD4 mice, which bear a transgenic B cell receptor that specifically binds the hen egg lysosome (HEL), to finally obtain GFP-*Bcl6*RD2^{MUT}-MD4 mice. Red fluorescent protein (RFP) mice were crossed to the WT MD4 background to generate RFP-MD4 mice. Naive B cells from GFP-*Bcl6*RD2^{MUT}-MD4 and RFP-WT-MD4 mice (at a 1:1 ratio) were transferred together with cyan fluorescent protein (CFP) expressing ovalbumin (OVA)-specific T cells to recipients, which were then immunized at the footpad with HEL-conjugated ovalbumin (HEL-OVA) in complete Freund's adjuvant (CFA) 2 days later (summarized in Figure 4A). This protocol ensured the

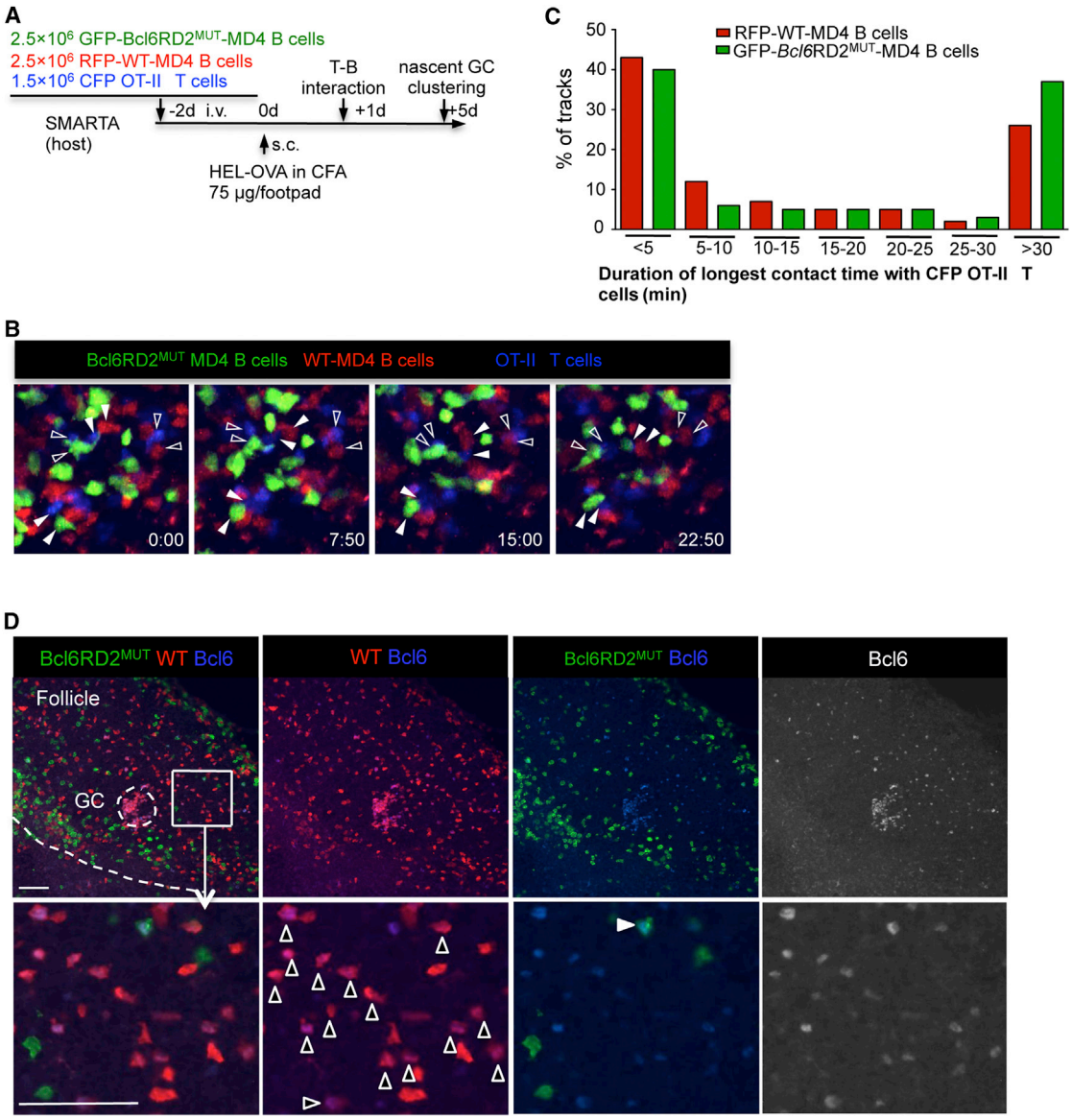

Figure 4. *Bcl6*RD2^{MUT} B Cells Exhibit Normal Contacts with Cognate T Helper Cells but Fail to Cluster into Nascent GCs

(A) Schematic outline of experimental approach.

(B) Time lapse images of CFP-OT-II T cells interacting with WT RFP-MD4 B cells and GFP-*Bcl6*RD2^{MUT}-MD4 B cells showing the tracks of motile T and B cells in conjugate pairs (see also Movies S1 and S2). Time is shown in minutes:seconds.

(C) Distribution of T-B cell contact durations of a representative experiment described in the Experimental Procedures.

(D) Bcl6 staining in sections of draining popliteal lymph nodes 5 days after immunization. Nascent GC is identified as the Bcl6^{hi} cell cluster (blue or white) and is highlighted by the open circle. A representative region close to the GC is boxed and shown in the bottom panel. Open and filled arrows indicate Bcl6^{hi} WT B cells and *Bcl6*RD2^{MUT} B cells, respectively. Scale bars, 50 μm.

specific recruitment of MD4 B cells to the GC formation pathway at the expense of the recipient B cell pool. SMARTA T cell receptor (TCR) transgenic mice were used as recipients to eliminate the endogenous T cell response to OVA. One day after immunization, time-resolved intravital imaging of adoptively transferred fluorescent cells within popliteal lymph nodes (LNs) was performed. Like WT B cells, *Bcl6*RD2^{MUT} B cells relocated to the periphery of B cell follicles and interfollicular zones (Figure 4B; Movies S1 and S2). Moreover, analysis of T-B cell contact times in vivo indicated that the duration of such interactions by *Bcl6*RD2^{MUT} B cells are comparable to that observed among WT B cells, typically lasting longer than 30 min and often for the duration of the imaging time period (Figures 4B and 4C; Movies S1 and S2).

*Bcl6*RD2^{MUT} B Cells Failed to Form Nascent GC Clusters

After immunization and initial cognate contact with T helper cells, some antigen-specific B cells proceed toward pre-GC B cell

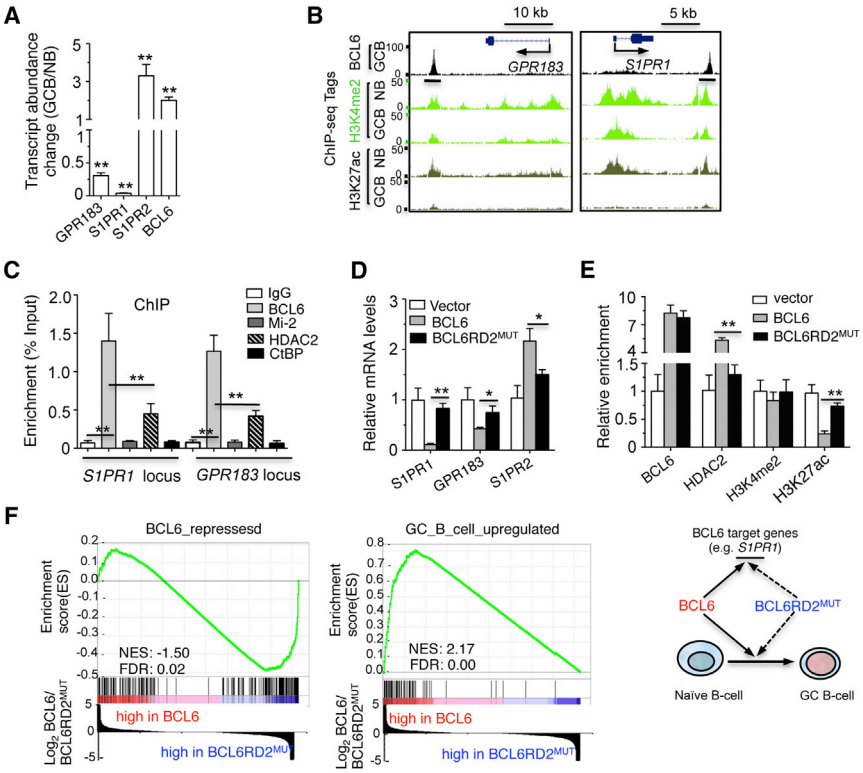

Figure 5. The BCL6 RD2 Domain Recruits HDAC2 to Repress *S1PR1* and *GPR183*

(A) Relative transcript abundance of *S1PR1*, *S1PR2*, and *GPR183* in human tonsillar GC B cells (GCB) compared with naive B cells (NB) after normalization of *HPRT*.

(B) ChIP-seq tags (y axis) are shown as a histogram for the enrichment of BCL6, H3K4me2, and H3K27ac in GC B cells and naive B cells for *S1PR1* and *GPR183* loci.

(C) Enrichment of indicated proteins at *S1PR1* and *GPR183* loci in human tonsillar GC B cells.

(D–F) OCI-LY1 cells stably expressing a control vector, siRNA-resistant BCL6 or BCL6RD2^{MUT} were transfected with *BCL6* siRNA#1 for 2 days. Relative transcript abundance of indicated genes (D) and fold change of enrichment of indicated proteins or histone marks at the *S1PR1* locus (E) were calculated compared with vector. Data are representative of three independent experiments. *$p < 0.05$ and **$p < 0.01$ (two-tailed t test). (F) GSEA of the gene-expression profiles of BCL6 and BCL6RD2^{MUT}-expressing OCI-LY1 cells for BCL6_repressed and GC_B_cell_upregulated gene sets. FDR, false discovery rate (q value); NES, normalized enrichment score. The cartoon illustrates that that RD2 mutant BCL6 is deficient in repressing many BCL6 target genes and deficient in enabling the GC B cell transcriptional program as compared with WT BCL6.

differentiation, characterized by upregulation of Bcl6 protein in the outer follicle, and finally coalesce and form small GC clusters in the follicle center 4–5 days after immunization (Kerfoot et al., 2011; Kitano et al., 2011). We next examined the ability of transferred antigen-specific *Bcl6*RD2^{MUT} B cells to form Bcl6^{hi} pre-GC B cells and GC structures in SMARTA TCR transgenic mice at day 5 after immunization (Figure 4A). As expected, WT RFP-MD4 B cells formed PNA^{+} GC clusters within follicles on day 5 after immunization (Figure S4B). WT Bcl6^{hi} RFP-MD4 B cells were predominantly found within GC and also in the region around GC (Figure 4D). In contrast, Bcl6^{hi} GFP-*Bcl6*RD2^{MUT}-MD4 B cells failed to self-aggregate or join GC structures, although they remained Ki67^{+}, and instead appeared randomly distributed (Figure 4D; Figure S4C). Similar to WT B cells, Ki67^{+} *Bcl6*RD2^{MUT}-B cells were also observed within the medullary cords and the periphery of follicles (data not shown), including the area adjacent to the subcapsular sinus, previously shown to support the extrafollicular formation of plasmablasts (Kerfoot et al., 2011).

The Bcl6 RD2 Domain Specifically Controls Genes Involved in B Cell Trafficking

The formation of GCs requires coordinated differential expression of specific lymphocyte trafficking factors. In murine B cells, downregulation of *Gpr183* (also known as *Ebi2*) is important for the clustering of pre-GC B cells within follicle centers (Gatto et al., 2009; Pereira et al., 2009). Upregulation of S1pr2 confines GC B cells within GCs (Green et al., 2011). S1pr1 enables B cell trafficking (Cinamon et al., 2004), and low S1pr1 levels in GC B cells were suggested to enable their retention within follicles (Green et al., 2011). Differential expression of these factors between murine GC and follicular B cells has been reported (Green et al., 2011). We also observed a similar expression pattern in human GC and follicular B cells (Figure 5A). Thus, we asked whether the BCL6 RD2 domain controls expression of these factors.

Analysis of chromatin immunoprecipitation sequencing (ChIP-seq) data (Béguelin et al., 2013; Huang et al., 2013) showed that BCL6 binds to distal regulatory sites associated with the *GPR183* and *S1PR1* genes, respectively (Figure 5B). Both these binding sites carry classical enhancer marks: histone 3 lysine 27 acetylation (H3K27ac) and histone 3 lysine 4 dimethylation (H3K4me2) in naive B cells. In contrast, the active enhancer mark H3K27ac (Creyghton et al., 2010) was clearly reduced in the presence of BCL6 in GC B cells (Figure 5B), consistent with the reduced abundance of *GPR183* and *S1PR1* mRNA. QChIP assays for BCL6 repression complexes at the *S1PR1* and *GPR183* loci in primary human GC B cells showed that HDAC2 was specifically bound along with BCL6 at both the *S1PR1* and *GPR183* enhancer regions (Figure 5C). In contrast, the core NuRD component Mi-2 and CtBP were absent from these sites, although they still occupied their known binding sites with BCL6 at intron 3 of *PRDM1* for Mi-2 and with the BCL6 promoter for CtBP (Figure S5A).

Next, we performed functional assays in GC-derived lymphoma cells to study the transcriptional mechanism of the BCL6 RD2 domain. BCL6 knockdown in BCL6-dependent OCI-Ly1 lymphoma cells derepressed both *GPR183* and

S1PR1 ($p < 0.05$; Figure S5B) and resulted in upregulation of *S1PR2* (possibly an indirect effect since BCL6 is not known to activate genes). Ectopic expression of WT, but not RD2 mutant BCL6, recruited HDAC2 to the *S1PR1* locus in BCL6 null MutuIII cells (Figure S5C). BCL6 knockdown in OCI-LY1 cells impaired recruitment of HDAC2 to *S1PR1* and *GPR183* loci, with a consequent increase of H3K27 acetylation of both loci. (Figure S5D) HDAC2 knockdown also induced H3K27 acetylation at both of these loci in these cells (Figure S5D).

To confirm whether repression of *S1PR1* and *GPR183* is specifically dependent on the BCL6 RD2, we performed rescue experiments in which we introduced WT or RD2 mutant BCL6 using expression constructs insensitive to siRNA into OCI-LY1 cells in which endogenous BCL6 was depleted by small interfering RNA (siRNA) knockdown (Figure S5E). RD2 mutant BCL6 failed to repress S1PR1 and GPR183 expression (Figure 5D). Moreover, RD2 mutant BCL6 was unable to recruit HDAC2 and deacetylate H3K27 at the *S1PR1* locus as compared with WT BCL6 (Figure 5E). Similar results were observed in an additional GC-derived lymphoma cell line (Figure S5F). Finally, migration assays in GC-derived lymphoma cells revealed that S1PR1 inhibits S1PR2-induced migration in the presence or absence of chemotactic cytokine CXCL12 (Figure S5G), consistent with antagonistic functions of S1PR1 and S1PR2 in B cell trafficking. Overall, the data suggest that BCL6 RD2 domain-dependent recruitment of HDAC2 mediates silencing of S1PR1 and GPR183 and indirectly induces upregulation of S1PR2, contributing to the clustering of B cells within follicles.

The BCL6 RD2 Domain Regulates Gene Sets Linked to the GC Phenotype

To examine whether the BCL6 RD2 domain might regulate additional genes linked to the GC phenotype, we performed RNA sequencing to compare the gene expression profiles of endogenous BCL6-depleted OCI-LY1 cells rescued with either WT or RD2 mutant BCL6. Unsupervised hierarchical clustering showed that the WT BCL6 and RD2 mutant gene expression profiles were clearly distinct and distributed to distinct clusters (Figure S5H). Gene set enrichment analysis (GSEA) revealed that a canonical set of genes, known to be downregulated by BCL6 in B cell lymphoma cells (Shaffer et al., 2000), was significantly repressed in WT BCL6 versus RD2 mutant BCL6 (normalized enrichment score [NES] = −1.50, false discovery rate [FDR] = 0.02; Figure 5F). Conversely, a canonical GC B cell gene set, consisting of genes that are upregulated in GC B cells compared with other B cell types (Shaffer et al., 2001), was significantly enriched (NES = 2.17, FDR = 0.00) in WT BCL6 as compared with RD2 mutant BCL6 expressing B cells (Figure 5F). This result is consistent with the notion that the RD2 domain functions of BCL6 are required for B cells to acquire the GC phenotype.

The RD2 Domain Is Dispensable for the Anti-inflammatory Function of Bcl6

Bcl6$^{-/-}$ mice are born at sub-Mendelian frequency. The pups exhibit developmental delays and runted size (Dent et al., 1997; Fukuda et al., 1997; Ye et al., 1997). Within weeks they develop a fatal inflammatory syndrome driven by macrophage and Th2 cells (Mondal et al., 2010; Toney et al., 2000). In marked contrast, *Bcl6*RD2^{MUT} mice were born at the expected ratios, exhibited normal body weights (Figure 6A), and lived normal healthy lifespans. *Bcl6*RD2^{MUT} animals did not exhibit any evidence of tissue damage or cellular infiltrates upon histopathology exam of various target organs of the *Bcl6*$^{-/-}$ inflammatory disease including lungs (Figure 6B) and other organs (data not shown). Bcl6 represses expression of inflammatory chemokines such as *Ccl2*, *Ccl3*, *Ccl6*, *Ccl7*, and *Il-1a* in macrophages. The loss of Bcl6 results in marked upregulation of these genes in macrophages and splenic B cells, which is believed to contribute to the lethal *Bcl6*$^{-/-}$ phenotype (Shaffer et al., 2000; Toney et al., 2000). These inflammatory response genes were only minimally increased in resting or lipopolysaccharide (LPS)-stimulated macrophages from *Bcl6*RD2^{MUT} mice as compared with their WT counterparts (Figure 6C). Moreover, the abundance of these inflammatory cytokines in *Bcl6*RD2^{MUT} was comparable to WT B cells in either the resting or LPS-stimulated status (Shaffer et al., 2000) (Figure 6D). Finally, *Bcl6*$^{-/-}$ mice display a high proportion of Th2 and Th17 cells, which play a critical role in the manifestation of inflammatory disease (Mondal et al., 2010; Toney et al., 2000). This phenotype can be further induced and aggravated by immunization. However, *Bcl6*RD2^{MUT} mice displayed similar numbers of Th2 (1.6% ± 0.2% versus 2.0% ± 0.3%) and Th17 cells (0.5% ± 0.1% versus 0.6% ± 0.2%) to WT mice after immunization (Figure 6E), further demonstrating that Bcl6 RD2 domain functions are dispensable to the actions of BCL6 in repressing the inflammatory phenotype.

DISCUSSION

The development of GCs is a sequential and complex process, during which BCL6 serves as master regulator in multiple cell types (Goodnow et al., 2010; Klein and Dalla-Favera, 2008; McHeyzer-Williams et al., 2012), There are many unanswered questions regarding the mechanisms and stages at which Bcl6 controls this process. Dissection of these events is further complicated by the diverse functions of Bcl6 in B cells, T cells, etc., as well as the multifaceted biochemical mechanisms of action of Bcl6 (Bunting and Melnick, 2013).

After T cell-dependent antigen stimulation, Bcl6 protein begins to accumulate in pre-GC B cells in the outer follicle regions and is maintained at high levels within GC B cells (Kerfoot et al., 2011; Kitano et al., 2011). Its role in mature, established GCs is fairly well defined and is linked to its silencing of cell cycle, DNA damage sensing, and apoptosis checkpoint genes as well as repression of genes involved in terminal differentiation (Bunting and Melnick, 2013; Klein and Dalla-Favera, 2008). These well-known GC B cell functions are mediated through Bcl6 BTB domain-dependent recruitment of the SMRT, NCOR, and BCOR corepressors (Hatzi et al., 2013; Huang et al., 2013; Polo et al., 2004). In contrast, the significance of Bcl6 in B cells at the pre-GC stage has not been confirmed, and the molecular basis for Bcl6-mediated pre-GC B cell differentiation remains unknown. Our current data showing that the Bcl6 RD2 domain plays an essential role in pre-GC B cell differentiation and nascent GC formation thus significantly extends knowledge of how B cells adopt the GC fate under the control of a specific BCL6

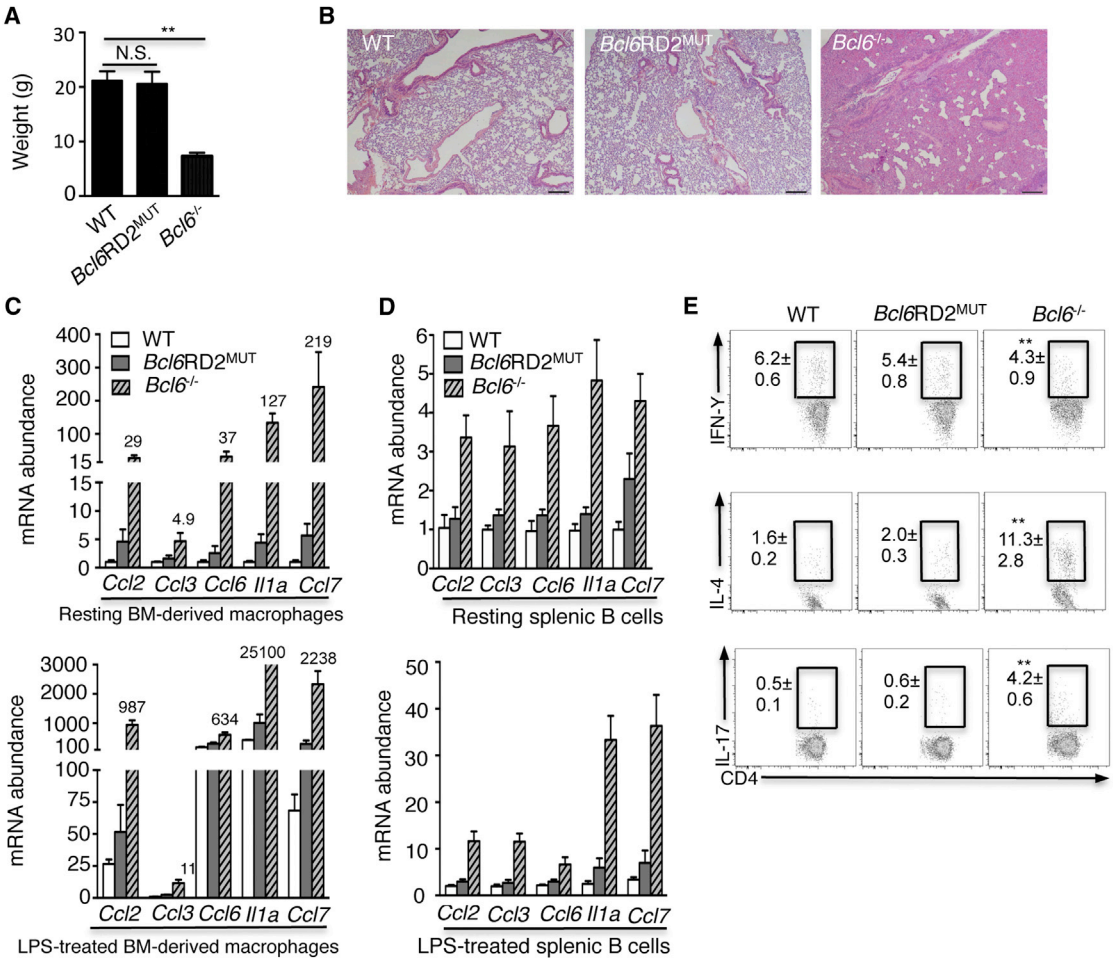

Figure 6. *Bcl6*RD2^{MUT} Mice Fail to Develop Macrophage and/or T_{H2} Driven Inflammatory Disease

(A) Body weight of indicated mice at 8 weeks of age (n = 6).

(B) Representative hematoxylin and eosin-stained lung sections from indicated mice. Scale bars, 200 μm.

(C and D) mRNA expression of indicated genes in resting or LPS-treated bone marrow-derived macrophages (C) and splenic B cells (D) from indicated mice (n = 3). Data were obtained from three independent experiments and are represented as fold-upregulation relative to WT resting cells after normalization with *Hprt*. Numbers adjacent to the error bars indicate fold induction.

(E) Percentage of IFNϒ, IL-4, and IL-17 secreting cells among CD4+ cells from indicated mice. The data shown indicate mean + SD from three mice. N.S., not significant; *p < 0.05, **p < 0.01, and ***p < 0.001 (two-tailed t test).

biochemical mechanism distinct from its known canonical function (Figure 4). The profound defect in early pre-GC differentiation in RD2-deficent B cells best explains the complete abrogation of GC formation in Bcl6 knockout mice and emphasizes the importance of Bcl6 in early GC B cell commitment.

The canonical BCL6 repressive mechanism of action in GC B cells is mediated by recruitment of the SMRT, NCOR, and BCOR corepressors to the BCL6 BTB domain (Hatzi and Melnick, 2014). However, we find that Bcl6 BTB mutant mice are still mostly capable of forming early GC clusters. This phenotype is in contrast to the complete abrogation of GC formation observed in BCL6 RD2 mutant mice. Hence, whereby BCL6 mediates early steps in commitment to the GC fate and clustering into nascent GCs through the RD2 domain, once GCs are established, Bcl6 is then required to maintain the proliferation and survival by repressing genes through its BTB domain. These findings suggest a model of sequential and biochemically distinct biological functions of BCL6 at different GC B cell developmental stages (Figure S6). It is also possible that the RD2 domain might also contribute to later events in established GCs such as regulation of terminal differentiation (Fujita et al., 2004; Parekh et al., 2007), although such functions cannot be assessed in the RD2 animal model developed here.

This pre-GC B cell differentiation deficiency caused by RD2 loss of function was explained at least in part by the finding that the BCL6 RD2 domain is required to repress expression of the key migration factors GRP183 and S1PR1. Downregulation of GRP183 is critically important for B cell migration into the follicle center (Gatto et al., 2009; Pereira et al., 2009). S1PR1 plays a key role in enabling B cell trafficking out of follicles (Cinamon

et al., 2004). Our finding that BCL6 directly represses these genes in GC cells suggests a role for BCL6 at an early stage of the GC response, whereby BCL6 can enable "capture" of B cells within follicles to enable their clustering. At the same time, S1PR2 upregulation in GC B cells confines them to an S1P-low niche within follicles (Green et al., 2011). We observed that S1PR1 overexpression promoted GC-type B cell migration and antagonized S1PR2 (Figure S5G). Taken together, the data suggest that dynamic regulation and equilibrium of S1PR1 and S1PR2 is a critical event in the early pre-GC phase of the humoral immune response, controlled at least in part through BCL6 direct binding and repression of S1PR1.

From a mechanistic standpoint, the BCL6 RD2 domain represses the *GPR183* and *S1PR1* loci by recruiting HDAC2, but not MTA3-NuRD, to suppress the enhancer activation mark H3K27ac at their distal regulatory elements. However, these data do not exclude the possibility that other as yet unknown corepressor proteins may bind with BCL6-HDAC2 repression complexes to these key target genes. Taken together with recent findings showing that BCL6 BTB domain corepressors distribute to different sets of genomic loci with unique functions in GC B cells (Hatzi et al., 2013), these data suggest that transcriptional programming by BCL6 is exquisitely compartmentalized through linkage of distinct biochemical functions to genes involved in specific immunological and biological functions.

In contrast to *Bcl6*$^{-/-}$ T cells, *Bcl6*RD2^{MUT} T cells were partially impaired in their ability to form GC-T_{FH} cells (Figure S6), which is somewhat similar to a hypomorphic defect observed in *Bcl6*$^{+/-}$ T cells (Yu et al., 2009). This defect is partially explained by the fact that RD2 mutant GC-T_{FH} cells exhibited reduced *IL-21* expression and increased *Blimp1*. Repression of *Blimp1* by BCL6 is known to critical for GC-T_{FH} cell differentiation and function (Johnston et al., 2009). IL-21 is expressed by GC-T_{FH} cell to promote GC B cell development and maintenance (Linterman et al., 2010; Zotos et al., 2010). Unlike *Bcl6*$^{-/-}$ mice, inflammatory responses and macrophage regulation were not significantly disrupted in *Bcl6*RD2^{MUT} mice. Neither loss of the BTB domain lateral groove nor the RD2 domain are sufficient to elicit deregulation of inflammatory signaling, which must instead be more reliant on other functions of Bcl6. The dominant mechanism may be linked at least in part to the previously reported competition with STAT proteins for binding to promoters of genes regulating inflammatory signaling (Dent et al., 1997; Huang et al., 2013) (Figure S6).

In conclusion, we identify the repressor function of the Bcl6 RD2 as a critical molecular mechanism required for early stages of GC B cell differentiation. Through recruitment of HDAC2 and perhaps additional cofactors, the RD2 domain mediates repression of genes that must be downregulated for BCL6 to commit to GC formation and form clusters within lymphoid follicles.

EXPERIMENTAL PROCEDURES

Animals

Mice were housed in the specific pathogen-free animal facility at the Weill Cornell Medical College and experiments performed using protocols approved by Institutional Animal Care and Use Committee. Generation of the *Bcl6*RD2^{MUT} knockin mouse and other animal are described in the Supplemental Information.

Bone Marrow Chimera Studies

Eight-week-old sublethally irradiated *Rag1*$^{-/-}$ mice were used as recipients. To generate mixed chimera (Figure 2A), 4 × 10^6 bone marrow cells from a mixture of WT CD45.1 and CD45.2 (WT, *Bcl6*$^{-/-}$, or *Bcl6*RD2^{MUT}) with a ratio of 1:1 were injected intravenously into recipients. To generate μMT chimera (Figure 3A), 4 × 10^6 bone marrow cells from a mixture of μMT and WT, *Bcl6*$^{-/-}$, or *Bcl6*RD2^{MUT} mice with a ratio of 4:1 were intravenously transferred into recipients. For generation of *Tcr*$^{-/-}$ chimeras (Figure 3D), recipients received a mixture of 80% bone marrow cells of *Tcrb*$^{-/-}$*Tcrd*$^{-/-}$ donors and 20% WT, *Bcl6*$^{-/-}$, or *Bcl6*RD2^{MUT}. Eight weeks after reconstruction, the recipients were immunized intraperitoneally (i.p.) with SRBCs (Cocalico Biologicals) for 10 days for analysis of GC formation, or the recipients were immunized i.p. with NP26-CGG (Biosearch Technologies) in Alum (Thermo Sciences) at 21 days for evaluation of antibody production.

Cell Isolation, Adoptive Transfers, and Immunizations

MD4-specific B cells were isolated from the spleens and lymph nodes of mice by immnomagnetic purification with the negative selection EasySep Mouse B Cell Enrichment Kit (StemCell Technologies). T cells were purified from the spleens and lymph nodes of OT-II mice with the negative selection EasySep CD4$^+$ T Cell Enrichment Kit (StemCell Technologies). For both intravital imaging and histology experiments (Figure 4), 2.5 × 10^6 GFP-*Bcl6*RD2^{MUT}-MD4 B cells, 2.5 × 10^6 RFP-WT-MD4$^+$ B cells, and 1.5 × 10^6 T cells were transferred for all time points. Cells were injected intravenously into SMARTA recipients that were immunized with 75 μg of HEl-OVA emulsified in CFA (Thermo Sciences) at 1.5 mg/ml in the right hind footpad.

Intravital Microscopy

The popliteal lymph nodes of anesthetized mice were imaged 1 day after immunization. Mice were initially anesthetized with an i.p. injection of a ketamine and xylazine mixture and were subsequently kept anesthetized with a nebulized isoflurane-O_2 gas mixture. Animals were immobilized on a custom-built stage, and the right popliteal lymph node was surgically prepared as previously described (Mempel et al., 2004). For imaging acquisition, an Olympus BX61WI fluorescence microscope with a 20×, 0.95 NA water immersion Olympus objective and dedicated single-beam LaVision TriM laser-scanning microscope (LaVision BioTec) was controlled by Inspector Pro software. The microscope was outfitted with a Chameleon Vision II Ti:Sapphire laser (Coherent) with pulse precompensation. Emission wavelengths of 390–480 nm (blue, CFP), 500–550 nm (green, GFP), and 565–665 nm (red, RFP) were collected with an array of three photomultiplier tubes (Hamamatsu). For 4D analysis of cell migration, stacks of 24 optical sections with 3 μm z-spacing were acquired every 30 s for 60–120 min with the laser tuned to a wavelength of 880 nm. Each xy plane spanned 400–500 μm in each dimension with a resolution of 0.977 μm per pixel.

Statistical Analysis

Student's t test was performed for statistical analysis. The software GraphPad Prism 5 was used for this analysis. A p value more than 0.05 is considered to be no significance.

Additional methods are provided in the Supplemental Experimental Procedures.

ACCESSION NUMBERS

The NCBI Gene Expression Omnibus accession number for RNaseq data sets reported in this paper is GSE58365.

SUPPLEMENTAL INFORMATION

Supplemental Information includes Supplemental Experimental Procedures, six figures, four tables, and two movies and can be found with this article online at http://dx.doi.org/10.1016/j.celrep.2014.07.059.

AUTHOR CONTRIBUTIONS

C.H. designed the experiments and interpreted data. C.H., A.H., and A.M. conceived the study and wrote the paper. C.H., D.G.G., C.M.C., Y.J., K.H., M.T., and K.D. performed experiments. T.H. provided important reagents.

ACKNOWLEDGMENTS

A.M. is supported by NCI R01 104348 and is also supported by the Burroughs Wellcome Foundation and Chemotherapy Foundation. A.H. and D.G.G. are supported by NIH grants R01AI080850 and R21AI101704. This research was initially supported by a March of Dimes Basil O'Connor Scholar Award (A.M.). This work was facilitated by the Sackler Center for Biomedical and Physical Sciences at Weill Cornell Medical College. We thank H. Ye from the Albert Einstein College of Medicine for sharing *Bcl6*$^{-/-}$ mice and P. Wade from NIH for providing anti-MTA3.

Received: November 9, 2013
Revised: July 2, 2014
Accepted: July 31, 2014
Published: August 28, 2014

REFERENCES

Allen, C.D., Okada, T., and Cyster, J.G. (2007). Germinal-center organization and cellular dynamics. Immunity *27*, 190–202.

Béguelin, W., Popovic, R., Teater, M., Jiang, Y., Bunting, K.L., Rosen, M., Shen, H., Yang, S.N., Wang, L., Ezponda, T., et al. (2013). EZH2 is required for germinal center formation and somatic EZH2 mutations promote lymphoid transformation. Cancer Cell *23*, 677–692.

Bereshchenko, O.R., Gu, W., and Dalla-Favera, R. (2002). Acetylation inactivates the transcriptional repressor BCL6. Nat. Genet. *32*, 606–613.

Bunting, K.L., and Melnick, A.M. (2013). New effector functions and regulatory mechanisms of BCL6 in normal and malignant lymphocytes. Curr. Opin. Immunol. *25*, 339–346.

Calado, D.P., Sasaki, Y., Godinho, S.A., Pellerin, A., Köchert, K., Sleckman, B.P., de Alborán, I.M., Janz, M., Rodig, S., and Rajewsky, K. (2012). The cell-cycle regulator c-Myc is essential for the formation and maintenance of germinal centers. Nat. Immunol. *13*, 1092–1100.

Chang, C.C., Ye, B.H., Chaganti, R.S., and Dalla-Favera, R. (1996). BCL-6, a POZ/zinc-finger protein, is a sequence-specific transcriptional repressor. Proc. Natl. Acad. Sci. USA *93*, 6947–6952.

Choi, Y.S., Kageyama, R., Eto, D., Escobar, T.C., Johnston, R.J., Monticelli, L., Lao, C., and Crotty, S. (2011). ICOS receptor instructs T follicular helper cell versus effector cell differentiation via induction of the transcriptional repressor Bcl6. Immunity *34*, 932–946.

Cinamon, G., Matloubian, M., Lesneski, M.J., Xu, Y., Low, C., Lu, T., Proia, R.L., and Cyster, J.G. (2004). Sphingosine 1-phosphate receptor 1 promotes B cell localization in the splenic marginal zone. Nat. Immunol. *5*, 713–720.

Creyghton, M.P., Cheng, A.W., Welstead, G.G., Kooistra, T., Carey, B.W., Steine, E.J., Hanna, J., Lodato, M.A., Frampton, G.M., Sharp, P.A., et al. (2010). Histone H3K27ac separates active from poised enhancers and predicts developmental state. Proc. Natl. Acad. Sci. USA *107*, 21931–21936.

Crotty, S. (2011). Follicular helper CD4 T cells (TFH). Annu. Rev. Immunol. *29*, 621–663.

Dent, A.L., Shaffer, A.L., Yu, X., Allman, D., and Staudt, L.M. (1997). Control of inflammation, cytokine expression, and germinal center formation by BCL-6. Science *276*, 589–592.

Duy, C., Yu, J.J., Nahar, R., Swaminathan, S., Kweon, S.M., Polo, J.M., Valls, E., Klemm, L., Shojaee, S., Cerchietti, L., et al. (2010). BCL6 is critical for the development of a diverse primary B cell repertoire. J. Exp. Med. *207*, 1209–1221.

Fujita, N., Jaye, D.L., Geigerman, C., Akyildiz, A., Mooney, M.R., Boss, J.M., and Wade, P.A. (2004). MTA3 and the Mi-2/NuRD complex regulate cell fate during B lymphocyte differentiation. Cell *119*, 75–86.

Fukuda, T., Yoshida, T., Okada, S., Hatano, M., Miki, T., Ishibashi, K., Okabe, S., Koseki, H., Hirosawa, S., Taniguchi, M., et al. (1997). Disruption of the Bcl6 gene results in an impaired germinal center formation. J. Exp. Med. *186*, 439–448.

Gatto, D., Paus, D., Basten, A., Mackay, C.R., and Brink, R. (2009). Guidance of B cells by the orphan G protein-coupled receptor EBI2 shapes humoral immune responses. Immunity *31*, 259–269.

Goenka, R., Barnett, L.G., Silver, J.S., O'Neill, P.J., Hunter, C.A., Cancro, M.P., and Laufer, T.M. (2011). Cutting edge: dendritic cell-restricted antigen presentation initiates the follicular helper T cell program but cannot complete ultimate effector differentiation. J. Immunol. *187*, 1091–1095.

Goodnow, C.C., Vinuesa, C.G., Randall, K.L., Mackay, F., and Brink, R. (2010). Control systems and decision making for antibody production. Nat. Immunol. *11*, 681–688.

Green, J.A., Suzuki, K., Cho, B., Willison, L.D., Palmer, D., Allen, C.D., Schmidt, T.H., Xu, Y., Proia, R.L., Coughlin, S.R., and Cyster, J.G. (2011). The sphingosine 1-phosphate receptor $S1P_2$ maintains the homeostasis of germinal center B cells and promotes niche confinement. Nat. Immunol. *12*, 672–680.

Hatzi, K., and Melnick, A. (2014). Breaking bad in the germinal center: how deregulation of BCL6 contributes to lymphomagenesis. Trends Mol. Med. *20*, 343–352.

Hatzi, K., Jiang, Y., Huang, C., Garrett-Bakelman, F., Gearhart, M.D., Giannopoulou, E.G., Zumbo, P., Kirouac, K., Bhaskara, S., Polo, J.M., et al. (2013). A hybrid mechanism of action for BCL6 in B cells defined by formation of functionally distinct complexes at enhancers and promoters. Cell Rep. *4*, 578–588.

Huang, C., Hatzi, K., and Melnick, A. (2013). Lineage-specific functions of Bcl-6 in immunity and inflammation are mediated by distinct biochemical mechanisms. Nat. Immunol. *14*, 380–388.

Johnston, R.J., Poholek, A.C., DiToro, D., Yusuf, I., Eto, D., Barnett, B., Dent, A.L., Craft, J., and Crotty, S. (2009). Bcl6 and Blimp-1 are reciprocal and antagonistic regulators of T follicular helper cell differentiation. Science *325*, 1006–1010.

Kerfoot, S.M., Yaari, G., Patel, J.R., Johnson, K.L., Gonzalez, D.G., Kleinstein, S.H., and Haberman, A.M. (2011). Germinal center B cell and T follicular helper cell development initiates in the interfollicular zone. Immunity *34*, 947–960.

Kitano, M., Moriyama, S., Ando, Y., Hikida, M., Mori, Y., Kurosaki, T., and Okada, T. (2011). Bcl6 protein expression shapes pre-germinal center B cell dynamics and follicular helper T cell heterogeneity. Immunity *34*, 961–972.

Klein, U., and Dalla-Favera, R. (2008). Germinal centres: role in B-cell physiology and malignancy. Nat. Rev. Immunol. *8*, 22–33.

Linterman, M.A., Beaton, L., Yu, D., Ramiscal, R.R., Srivastava, M., Hogan, J.J., Verma, N.K., Smyth, M.J., Rigby, R.J., and Vinuesa, C.G. (2010). IL-21 acts directly on B cells to regulate Bcl-6 expression and germinal center responses. J. Exp. Med. *207*, 353–363.

McHeyzer-Williams, M., Okitsu, S., Wang, N., and McHeyzer-Williams, L. (2012). Molecular programming of B cell memory. Nat. Rev. Immunol. *12*, 24–34.

Mempel, T.R., Henrickson, S.E., and Von Andrian, U.H. (2004). T-cell priming by dendritic cells in lymph nodes occurs in three distinct phases. Nature *427*, 154–159.

Mendez, L.M., Polo, J.M., Yu, J.J., Krupski, M., Ding, B.B., Melnick, A., and Ye, B.H. (2008). CtBP is an essential corepressor for BCL6 autoregulation. Mol. Cell. Biol. *28*, 2175–2186.

Mondal, A., Sawant, D., and Dent, A.L. (2010). Transcriptional repressor BCL6 controls Th17 responses by controlling gene expression in both T cells and macrophages. J. Immunol. *184*, 4123–4132.

Nurieva, R.I., Chung, Y., Martinez, G.J., Yang, X.O., Tanaka, S., Matskevitch, T.D., Wang, Y.H., and Dong, C. (2009). Bcl6 mediates the development of T follicular helper cells. Science *325*, 1001–1005.

Okada, T., Miller, M.J., Parker, I., Krummel, M.F., Neighbors, M., Hartley, S.B., O'Garra, A., Cahalan, M.D., and Cyster, J.G. (2005). Antigen-engaged B cells undergo chemotaxis toward the T zone and form motile conjugates with helper T cells. PLoS Biol. *3*, e150.

Parekh, S., Polo, J.M., Shaknovich, R., Juszczynski, P., Lev, P., Ranuncolo, S.M., Yin, Y., Klein, U., Cattoretti, G., Dalla Favera, R., et al. (2007). BCL6 programs lymphoma cells for survival and differentiation through distinct biochemical mechanisms. Blood *110*, 2067–2074.

Pereira, J.P., Kelly, L.M., Xu, Y., and Cyster, J.G. (2009). EBI2 mediates B cell segregation between the outer and centre follicle. Nature *460*, 1122–1126.

Polo, J.M., Dell'Oso, T., Ranuncolo, S.M., Cerchietti, L., Beck, D., Da Silva, G.F., Prive, G.G., Licht, J.D., and Melnick, A. (2004). Specific peptide interference reveals BCL6 transcriptional and oncogenic mechanisms in B-cell lymphoma cells. Nat. Med. *10*, 1329–1335.

Qi, H., Cannons, J.L., Klauschen, F., Schwartzberg, P.L., and Germain, R.N. (2008). SAP-controlled T-B cell interactions underlie germinal centre formation. Nature *455*, 764–769.

Seyfert, V.L., Allman, D., He, Y., and Staudt, L.M. (1996). Transcriptional repression by the proto-oncogene BCL-6. Oncogene *12*, 2331–2342.

Shaffer, A.L., Yu, X., He, Y., Boldrick, J., Chan, E.P., and Staudt, L.M. (2000). BCL-6 represses genes that function in lymphocyte differentiation, inflammation, and cell cycle control. Immunity *13*, 199–212.

Shaffer, A.L., Rosenwald, A., Hurt, E.M., Giltnane, J.M., Lam, L.T., Pickeral, O.K., and Staudt, L.M. (2001). Signatures of the immune response. Immunity *15*, 375–385.

Toney, L.M., Cattoretti, G., Graf, J.A., Merghoub, T., Pandolfi, P.P., Dalla-Favera, R., Ye, B.H., and Dent, A.L. (2000). BCL-6 regulates chemokine gene transcription in macrophages. Nat. Immunol. *1*, 214–220.

Victora, G.D., and Nussenzweig, M.C. (2012). Germinal centers. Annu. Rev. Immunol. *30*, 429–457.

Ye, B.H., Cattoretti, G., Shen, Q., Zhang, J., Hawe, N., de Waard, R., Leung, C., Nouri-Shirazi, M., Orazi, A., Chaganti, R.S., et al. (1997). The BCL-6 proto-oncogene controls germinal-centre formation and Th2-type inflammation. Nat. Genet. *16*, 161–170.

Yu, D., Rao, S., Tsai, L.M., Lee, S.K., He, Y., Sutcliffe, E.L., Srivastava, M., Linterman, M., Zheng, L., Simpson, N., et al. (2009). The transcriptional repressor Bcl-6 directs T follicular helper cell lineage commitment. Immunity *31*, 457–468.

Zotos, D., Coquet, J.M., Zhang, Y., Light, A., D'Costa, K., Kallies, A., Corcoran, L.M., Godfrey, D.I., Toellner, K.M., Smyth, M.J., et al. (2010). IL-21 regulates germinal center B cell differentiation and proliferation through a B cell-intrinsic mechanism. J. Exp. Med. *207*, 365–378.